

# Scalable quantum random-access memory with superconducting circuits

T. H. Kyaw,<sup>1</sup> S. Felicetti,<sup>2</sup> G. Romero,<sup>2</sup> E. Solano,<sup>2,3</sup> and L. C. Kwek<sup>1,4,5</sup>

<sup>1</sup>Centre for Quantum Technologies, National University of Singapore, 3 Science Drive 2, Singapore 117543

<sup>2</sup>Department of Physical Chemistry, University of the Basque Country UPV/EHU, Apartado 644, E-48080 Bilbao, Spain

<sup>3</sup>IKERBASQUE, Basque Foundation for Science, Alameda Urquijo 36, 48011 Bilbao, Spain

<sup>4</sup>Institute of Advanced Studies, Nanyang Technological University, 60 Nanyang View, Singapore 639673

<sup>5</sup>National Institute of Education, Nanyang Technological University, 1 Nanyang Walk, Singapore 637616

(Dated: December 6, 2024)

Quantum networks<sup>1,2</sup> play an important role in the implementation of quantum computing, communication and metrology<sup>3-5</sup>. Circuit quantum electrodynamics (QED)<sup>6-8</sup>, consisting of superconducting artificial atoms coupled to on-chip resonators, provides a prime candidate to implement<sup>9,10</sup> these networks due to their controllability and scalability. Furthermore, recent advances have also pushed the technology to the ultrastrong coupling (USC) regime of light-matter interaction<sup>11-13</sup>, where the qubit-cavity coupling strength reaches a considerable fraction of the cavity frequency. Here, we propose the implementation of a scalable quantum random-access memory (QRAM) architecture based on a circuit QED network, whose edges operate in the USC regime. In particular, we study the storage and retrieval of quantum information in a parity-protected quantum memory and propose quantum interconnects<sup>5</sup> in experimentally feasible schemes. Our proposal may pave the way for novel quantum memory applications ranging from entangled-state cryptography<sup>14,15</sup>, teleportation<sup>16</sup>, purification<sup>17-19</sup>, fault-tolerant quantum computation<sup>20</sup>, to quantum simulations.

In distributed quantum information processing, quantum processors (QPs) are part of a quantum network and they may exchange data with one another via classical<sup>21</sup> or quantum<sup>5</sup> communication channels. Within the network, we envisage central QPs which distribute partial quantum information to other connected QPs. Each of these secondary QPs runs on a partial input, which may be independent of each other, correlated or entangled with other partial inputs. After the computation is completed, the central QPs store the global information by collecting partial outputs from secondary QPs. A subsequent step to the above data processing is the ability to store and retrieve quantum information into and from a QRAM. In our proposal, a qubit-cavity system that operates in the USC regime, located at the edges of a quantum network, and linked by coplanar waveguide resonators (CWR), is used as a quantum memory device. This configuration has two-fold benefits over a network of quantum nodes linked by classical channels. First, the fully quantum network provides an exponentially larger state space<sup>5</sup>. Second, they present a potentially powerful means to overcome size-scaling and error-correlation problems that would in turn limit the size of a quantum computer<sup>22</sup>.

Here, we show that circuit QED architectures operating at the ultrastrong coupling regime may represent a valuable platform to store quantum information. In this regime, the qubit-

cavity system exhibits a parity ( $Z_2$ ) symmetry and its dynamics is governed by the Rabi Hamiltonian<sup>23</sup>

$$H_{\text{Rabi}} = \frac{\hbar\omega_{eg}}{2}\sigma_z + \hbar\omega_{\text{cav}}a^\dagger a + \hbar\Omega\sigma_x(a + a^\dagger), \quad (1)$$

where  $\omega_{eg}$ ,  $\omega_{\text{cav}}$ , and  $\Omega$  stand for the qubit frequency, cavity frequency, and the qubit-cavity coupling strength, respectively. In addition,  $a(a^\dagger)$  is the bosonic annihilation(creation) operator, and  $\sigma_{x,z}$  are the Pauli matrices of the qubit. A noticeable feature of Hamiltonian (1) is that for ratios  $\Omega/\omega_{\text{cav}} \gtrsim 0.8$ , the ground and first excited states can be approximated as

$$\begin{aligned} |\psi_G\rangle &\simeq \frac{1}{\sqrt{2}}(|-\alpha\rangle|+\rangle - |\alpha\rangle|-\rangle), \\ |\psi_E\rangle &\simeq \frac{1}{\sqrt{2}}(|-\alpha\rangle|+\rangle + |\alpha\rangle|-\rangle), \end{aligned} \quad (2)$$

where  $|\alpha\rangle$  is a coherent state for the cavity field with amplitude  $|\alpha| = \Omega/\omega_{\text{cav}}$ , and  $|\pm\rangle = (|e\rangle \pm |g\rangle)/\sqrt{2}$  are the eigenstates of  $\sigma_x$ . The states  $|\psi_{G/E}\rangle$  form a parity protected qubit<sup>24</sup>

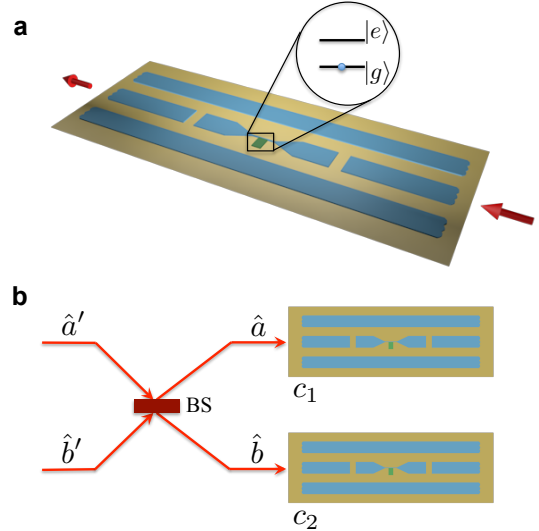


FIG. 1. Schematic of circuit-QED design for storage and retrieval of an unknown single- and two-qubit states. **a**, A USC edge, composed of a qubit-cavity system operating at the USC regime. **b**, Two bosonic modes  $\hat{a}'$  and  $\hat{b}'$  each carrying a single photon, come in from each arm and pass through a beam splitter (BS) implemented by a SQUID device to form an entangled state. The latter state may be stored in the USC qubits located at edges apart.

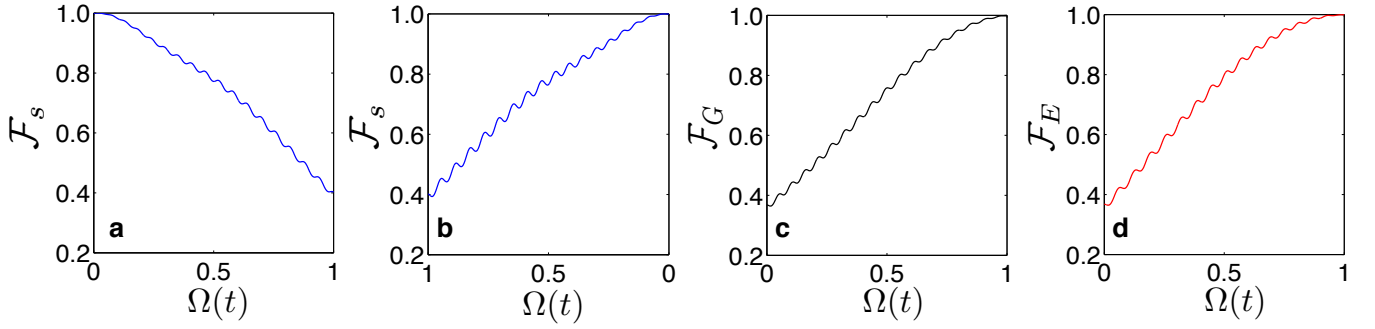


FIG. 2. **Storage and retrieval processes.** **a**, Storage process for a quantum state  $|\psi_s\rangle = \alpha_F|\psi_0\rangle + \beta_F|\psi_1\rangle$ . **b**, retrieval process. In both cases, we plot the fidelity between the initial  $|\psi_s\rangle$  and the instantaneous state  $|\psi(t)\rangle$ , i.e.,  $\mathcal{F}_s = |\langle\psi_s|\psi(t)\rangle|^2$ . Any arbitrary state  $|\psi\rangle = u|\psi_0\rangle + v|\psi_1\rangle$  can be stored and retrieved with unit fidelity. **c**, Fidelity between the approximated ground state in equation (2) and the instantaneous ground state  $\mathcal{F}_G = |\langle\psi_G|\psi_G(t)\rangle|^2$ . **d**, Fidelity between the approximated first excited state in equation (2) and the instantaneous first excited state  $\mathcal{F}_E = |\langle\psi_E|\psi_E(t)\rangle|^2$ . For all simulations we have fixed the system parameters as  $\omega_{\text{cav}} = 1$ ,  $\omega_{eg} = 0.1 \omega_{\text{cav}}$ ,  $\Omega_0 = \omega_{\text{cav}}$ , and the total evolution  $T = 105/\omega_{\text{cav}}$ .

whose coherence time is about  $\tau_{\text{coh}} \gtrsim 10^5/\omega_{eg}$ . We propose a protocol that allows storage and retrieval of quantum information from this qubit, by adiabatically tuning the qubit-cavity coupling strength from the Jaynes-Cummings regime to the USC regime. In addition, this scheme allows us to propose a quantum network whose edges operate in the USC regime of light-matter interaction.

In particular, we propose USC edges (see Fig. 1a) that can be designed by the flux-qubit architecture presented in reference<sup>25</sup>, which provides a tunable qubit-cavity coupling strength and the ultrastrong coupling regime. Furthermore, quantum interconnects in between the USC edges can be implemented by means of superconducting quantum interference devices (SQUIDs) at the nodes of the quantum network, see Fig 4a. The latter will allow us to selectively address pairwise interaction between non degenerate microwave CWR, so that quantum signals consisting of single photons may propagate across the network (see Supplementary Information).

The storage of quantum information into the USC edges involves two steps. Firstly, at the initial time  $t = 0$ , the qubit-cavity coupling strength is tuned to reach the strong coupling regime ( $\Omega/\omega_{\text{cav}} \ll 1$ ) which is described by the Jaynes-Cummings (JC) dynamics, and the qubit is decoupled from the cavity (Fig. 1a) in the off resonant regime ( $\omega_{eg} \gg \omega_{\text{cav}}$ ). In this case, the ground and the first excited states of the qubit-cavity system are  $|\psi_0\rangle = |g\rangle \otimes |0\rangle$  and  $|\psi_1\rangle = |e\rangle \otimes |0\rangle$ , respectively. Here, the states  $|g\rangle$  and  $|e\rangle$  stand for the ground and the excited states of the qubit, and  $|0\rangle$  stands for the vacuum state of the cavity. Suppose the qubit is initially prepared in  $|g\rangle$ , so the qubit-cavity system is in the state  $|\psi_0\rangle$ . When a qubit in the unknown state  $|\Psi_F\rangle = \alpha_F|0_F\rangle + \beta_F|1_F\rangle$  enters the QRAM from a specific colored node of the integrated QP (see Fig. 4b), the information is encoded in the flux qubit such that the qubit-cavity system is eventually prepared in the state  $|\psi_s\rangle = (\alpha_F|g\rangle + \beta_F|e\rangle) \otimes |0\rangle$ .

Secondly, we adiabatically switch on the qubit-cavity coupling until the system reaches the USC regime. For simplicity, we consider a linear adiabatic switching scheme such that  $\Omega(t) = (\cos(f) - \Delta f \sin(f)t/T)\Omega_0$ , with  $T$  the to-

tal evolution time, and  $f, \Delta f$  are parameters that depend on some external magnetic flux (see Methods). In Fig. 2a,b, we show the storage and retrieval processes for a quantum state  $|\psi_s\rangle = \alpha_F|\psi_0\rangle + \beta_F|\psi_1\rangle$ . The same simulation shows that the ground state  $|\psi_0\rangle$  and the first excited state  $|\psi_1\rangle$  adiabatically follow the instantaneous eigenstates such that  $|\psi_0\rangle \rightarrow |\psi_G\rangle$  and  $|\psi_1\rangle \rightarrow |\psi_E\rangle$ , see Fig. 2c,d. For all simulations we choose the total evolution time such that we reach a maximum fidelity at  $t = T$ . In this way, one can encode quantum information in the parity protected basis and decode it back by adiabatically switching the qubit-cavity coupling strength.

We stress that the time for storage and retrieval of quantum information is several order of magnitude faster than the coherence time of the parity protected qubit, which is about  $T_{\text{coh}} \sim 40 \mu\text{s}$  for a coupling strength  $\Omega_0/\omega_{eg} \sim 1.5$ <sup>24</sup>. For instance, if we consider a flux qubit with energy  $\omega_{eg}/2\pi \sim 2$  GHz, and a cavity of frequency  $\omega_{\text{cav}}/2\pi \sim 5$  GHz, the qubit-cavity system reaches the USC regime with  $\Omega_0/\omega_{\text{cav}} = 0.6$ . For the linear adiabatic switching scheme with the above parameters, we estimate total time for storage/retrieval of a qubit is about  $\bar{T} \approx 2 - 8$  ns.

To achieve unit fidelity in storing and retrieving a superposed state  $|\psi_s\rangle = \alpha_F|\psi_0\rangle + \beta_F|\psi_1\rangle$ , the state  $|\tilde{\psi}\rangle = \alpha_F|\psi_G\rangle + \beta_F|\psi_E\rangle$  is desired at the end of an adiabatic evolution. However, a resultant state after the evolution time  $\tau$  becomes  $|\tilde{\psi}(T)\rangle = \alpha_F|\psi_G(T)\rangle + \beta_F e^{i\theta(T)}|\psi_E(T)\rangle$ , with a relative phase  $\theta(T)$  which comes from the dynamical and geometrical effects<sup>26</sup>. In this sense, we need to keep track of the relative phase for the storage and retrieval processes. In order to find out which phase  $\theta(t)$  optimizes the storage processes, in Fig. 3, we plot the fidelity  $\mathcal{F}(\Omega, \theta) = |\langle\tilde{\psi}|\psi(t)\rangle|^2$  between the state  $|\tilde{\psi}\rangle = \alpha_F|\psi_G\rangle + \beta_F e^{i\theta}|\psi_E\rangle$  and the state  $|\psi(t)\rangle$ , which has adiabatically evolved from the initial state  $|\psi_s\rangle = \alpha_F|\psi_0\rangle + \beta_F|\psi_1\rangle$ . In this simulation, we consider  $\theta \in [0, 2\pi]$  versus the qubit-cavity coupling strength  $\Omega(t)$  for two different total evolution time  $T = 105/\omega_{\text{cav}}$  (Fig. 3a), and  $T = 120/\omega_{\text{cav}}$  (Fig. 3b). White lines show the phase  $\theta_{\text{opt}}$  which optimizes the fidelity  $\mathcal{F}$  for both cases. Notice that the maximum fidelity and the optimal phase  $\theta$  depend strongly on

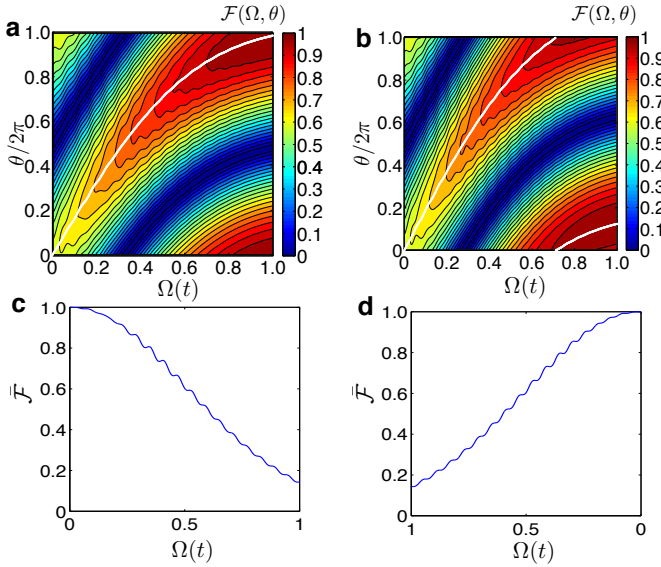


**FIG. 3. Relative phase and optimized fidelity. Storage and retrieval processes for an entangled state.** Contour plots of the fidelity  $\mathcal{F} = |\langle \tilde{\psi} | \psi(t) \rangle|^2$  between the state  $|\tilde{\psi}\rangle = \alpha_F |\psi_G\rangle + \beta_F e^{i\theta} |\psi_E\rangle$  and the state  $|\psi(t)\rangle$ , which has adiabatically evolved from the initial state  $|\psi_s\rangle = \alpha_F |\psi_0\rangle + \beta_F |\psi_1\rangle$ . **a**, The total evolution time is set to  $T = 105/\omega_{\text{cav}}$ . **b**, The evolution time is  $T = 120/\omega_{\text{cav}}$ . For the above cases, the black lines stand for the phase which maximized the fidelity  $\mathcal{F}$ . In these simulations, the parameters are  $\omega_{\text{cav}} = 1$ ,  $\omega_{eg} = 0.1 \omega_{\text{cav}}$ , and  $\Omega_0 = \omega_{\text{cav}}$ . **c**, Storage process for an entangled state  $|\Psi_0\rangle = \frac{1}{\sqrt{2}}(|ge\rangle + |eg\rangle) \otimes |00\rangle_{c_1 c_2}$ . **d**, retrieval process. In both cases, we plot the fidelity between the initial state  $|\Psi_0\rangle$ , and the instantaneous state  $|\psi(t)\rangle$ ,  $\bar{\mathcal{F}} = |\langle \Psi_0 | \psi(t) \rangle|^2$ . In this simulation we have chosen  $\omega_{\text{cav}} = 1$ ,  $\omega_{eg} = 0.1 \omega_{\text{cav}}$ ,  $\Omega_0 = \omega_{\text{cav}}$ , and the evolution time  $T = 105/\omega_{\text{cav}}$ .

the system parameters and the total evolution time  $T$ . Thus, we require, for each USC edge, to find out the parameter  $T$  which gives maximum fidelity only once. Once  $T$  is known, an edge can always be operated at that specific parameter for storing and retrieving unknown quantum states. Therefore, the time  $T$  might be a benchmark to characterize our potential USC quantum memory devices (QMDs), in the same way as hard disk drives (HDDs) of the current classical computer are being characterized by their seek time and latency.

It is noteworthy that our protocol allows storing of entangled states in separated USC edges, see Fig. 1b. To test such process, an entangled state of two USC edges can be created by letting two bosonic fields to interact via the SQUID device, simulating a Hong-Ou-Mandel (HOM) setup<sup>27</sup> as shown in Fig. 1b. Let us suppose that we have an initial state  $|\psi_0\rangle = |0\rangle_{\hat{a}'} |1\rangle_{\hat{b}'}$ . After experiencing a beam splitter (BS) interaction, we have the entangled state  $|\psi_0'\rangle = \frac{1}{\sqrt{2}}(|0\rangle_{\hat{a}} |1\rangle_{\hat{b}} + |1\rangle_{\hat{a}} |0\rangle_{\hat{b}})$ . The two photons enter two different cavities  $c_1$  and  $c_2$ , each containing of a flux qubit prepared in its ground state. The latter process allows the cavities to be prepared in the state  $|\bar{\Psi}_0\rangle = \frac{1}{\sqrt{2}}(|0\rangle_{c_1} |1\rangle_{c_2} + |1\rangle_{c_1} |0\rangle_{c_2}) \otimes |gg\rangle$ . Following the same procedure to store a single qubit by tuning the Jaynes-

Cummings dynamics, we tune the qubits towards resonance with its respective cavity such that the state becomes  $|\Psi_0\rangle = \frac{1}{\sqrt{2}}(|ge\rangle + |eg\rangle) \otimes |00\rangle_{c_1 c_2}$ . Therefore, we can store the entangled state  $|\Psi_0\rangle$  onto two separated edges. Following the adiabatic process described above, the state can be mapped onto a parity protected state  $|\bar{\Psi}_0\rangle = \frac{1}{\sqrt{2}}(|\psi_G\rangle |\psi_E\rangle + |\psi_E\rangle |\psi_G\rangle)$ . We show the quantum state fidelity of the storage and retrieval processes for the entangled state  $|\Psi_0\rangle$  in Fig. 3c,d.

In conclusion, we have presented the basic tools for building a QRAM based on a circuit QED architecture that operates at the USC regime of light-matter interaction. The storage/retrieval process for unknown quantum states, be single qubit or entangled two-qubit states, can be accomplished by adiabatically switching on/off the qubit-cavity coupling strength. Our proposal aims to develop a large quantum network such as in Fig. 4, where each edge of the network is constituted by a qubit-cavity system operating at the USC regime that exhibits a  $Z_2$  symmetry, and each node is connected to a superconducting quantum interference device that allows to switch on/off the interaction between neighboring microwave cavities<sup>29</sup>. In this sense, we envision a full-fledged distributed quantum information platform involving QRAM and QPs in an integrated manner.

## METHODS

### Switchable qubit-cavity coupling strength

In a circuit QED architecture formed by a flux qubit galvanically coupled to a inhomogeneous cavity (see Supplementary Information), the Hamiltonian that describes the dynamics reads

$$H = \frac{\hbar\omega_{eg}}{2} \sigma_z + \hbar\omega_{\text{cav}} a^\dagger a + H_{\text{int}}, \quad (3)$$

with the effective tunable interaction Hamiltonian

$$H_{\text{int}} = -2E_J \beta \cos\left(\pi \frac{\phi_{\text{ext}}}{\phi_0}\right) \sum_{n=1,2} (\Delta\psi)^n \sum_{\mu=x,y,z} c_\mu^{(n)} \sigma_\mu, \quad (4)$$

where  $E_J$  is Josephson energy,  $\beta$  is a parameter that depends on the Josephson junctions size,  $\phi_0 = h/2e$  is the flux quantum, and  $\phi_{\text{ext}}$  is an external flux that can be applied to a superconducting loop, this in turn allows to switch on/off the qubit-cavity coupling strength. In addition,  $\Delta\psi$  stands for the phase slip shared by the cavity and the flux qubit, and the coefficients  $c_\mu^{(n)}$  can be tuned at will via additional external fluxes (see Supplementary Information).

### Adiabatic evolution

From equations (7) and (8) we can obtain the effective system Hamiltonian  $H = \frac{\hbar\omega_{eg}}{2} \sigma_z^j + \hbar\omega_{\text{cav}} a^\dagger a + (\cos(f) - \Delta f \sin(f)t/T) \Omega_0 \sigma_x^j (a^\dagger + a)$ , if we consider an external flux that varies linearly with time according to  $\phi_{\text{ext}} = \bar{\phi}_0 + \Delta\phi t/T$  with  $\bar{\phi}_0$  an offset flux, and  $\Delta\phi$  a small flux amplitude. It is noteworthy that all our simulations have been presented assuming no losses either qubits or cavities. Nonetheless, this task can be carried out by studying the Bloch-Redfield master equation (see Supplementary Information).

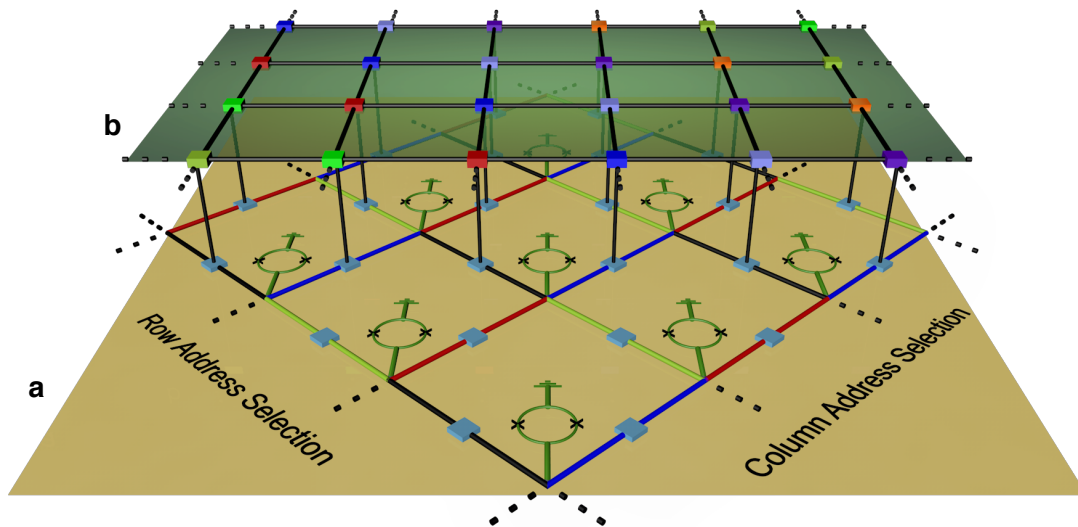


FIG. 4. **a, A scalable QRAM.** The light-matter interfaces operating at the ultrastrong coupling regime may be envisioned as a set of microwave cavities connected, at the nodes, by SQUID devices that allow to switch on/off the cavity-cavity interaction. Notice that each cavity is represented with different colors (red, black, blue and green) that stand for different lengths to assure the manipulation of specific pairwise interactions (see Supplementary Information). In addition, on each edge of the quantum network, there is a USC entity (blue square) to store an arbitrary quantum information in a specific location by addressing fluxes through the row and column SQUIDs. **b, Integrated quantum processor.** A 2D cavity grid with a qubit distribution (rectangular boxes) represented in various colors is shown here. It was previously shown<sup>28</sup> that such a cavity grid may provide a scalable fault-tolerant quantum computing architecture with minimal swapping overhead. We envisage that all the necessary quantum processing is done in the integrated QP while storage/retrieval of information is done in the QRAM.

- <sup>1</sup> Bouwmeester, D., Ekert, A. & Zeilinger, A. *The Physics of Quantum Information* (Springer, Berlin, 2000).
- <sup>2</sup> Cirac, J. I., Zoller, P., Kimble, H. J. & Mabuchi, H. Quantum state transfer and entanglement distribution among distant nodes in a quantum network. *Phys. Rev. Lett.* **78**, 3221 (1997).
- <sup>3</sup> Bennett, C. H., Brassard, G. & Ekert, A. K. Quantum cryptography. *Sci. Am.* **267**(4), 50-57 (October 1992).
- <sup>4</sup> Giovannetti, V., Lloyd, S. & Maccone, L. Quantum-enhanced measurements: beating the standard quantum limit. *Science* **306**, 1330-1336 (2004).
- <sup>5</sup> Kimble, H. J. The quantum internet. *Nature* **453**, 1023-1030 (2008).
- <sup>6</sup> Blais, A., Huang, R. S., Wallraff, A., Girvin, S. M. & Schoelkopf, R. J. Cavity quantum electrodynamics for superconducting electrical circuits: An architecture for quantum computation. *Phys. Rev. A* **69**, 062320 (2004).
- <sup>7</sup> Chiorescu, I. et al. Coherent dynamics of a flux qubit coupled to a harmonic oscillator. *Nature* **431**, 159-162 (2004).
- <sup>8</sup> Wallraff, A. et al. Strong coupling of a single photon to a superconducting qubit using circuit quantum electrodynamics. *Nature* **431**, 162-167 (2004).
- <sup>9</sup> Wenner, J. et al. Catching Shaped Microwave Photons with 99.4% Absorption Efficiency. Preprint at <http://arxiv.org/abs/arXiv:1311.1180> (2013).
- <sup>10</sup> Flurin, E. et al. Superconducting quantum node for entanglement and storage of microwave radiation. Preprint at <http://arxiv.org/abs/arXiv:1401.5622> (2014).
- <sup>11</sup> Bourassa, J. et al. Ultrastrong coupling regime of cavity QED with phase-biased flux qubits. *Phys. Rev. A* **80**, 032109 (2009).
- <sup>12</sup> Niemczyk, T. et al. Circuit quantum electrodynamics in the ultrastrong-coupling regime. *Nature Phys.* **6**, 772-776 (2010).
- <sup>13</sup> Forn-Díaz, et al. Observation of the Bloch-Siegert shift in a qubit-oscillator system in the ultrastrong coupling regime. *Phys. Rev. Lett.* **105**, 237001 (2010).
- <sup>14</sup> Bennett, C. H. Quantum information and computation. *Phys. Today* **48**(10), 24-30 (October 1995).
- <sup>15</sup> Ekert, A. K. Quantum cryptography based on Bell's theorem. *Phys. Rev. Lett.* **67**, 661 (1991).
- <sup>16</sup> Bennett, C. H. et al. Teleporting an unknown quantum state via dual classical and Einstein-Podolsky-Rosen channels. *Phys. Rev. Lett.* **70**, 1895 (1993).
- <sup>17</sup> Bennett, C. H. et al. Purification of Noisy Entanglement and Faithful Teleportation via Noisy Channels. *Phys. Rev. Lett.* **76**, 722 (1996).
- <sup>18</sup> Deutsch, D. et al. Quantum Privacy Amplification and the Security of Quantum Cryptography over Noisy Channels. *Phys. Rev. Lett.* **77**, 2818 (1996).
- <sup>19</sup> Gisin, N. Hidden quantum nonlocality revealed by local filters. *Phys. Lett. A* **210**, 151 (1996).
- <sup>20</sup> Nigg, S. E., & Girvin, S. M. Stabilizer Quantum Error Correction Toolbox for Superconducting Qubits. *Phys. Rev. Lett.* **110**, 243604 (2013).
- <sup>21</sup> Cirac, J. I., Ekert, A. K., Huelga, S. F., & Macchiavello, C. Distributed quantum computation over noisy channels. *Phys. Rev. A* **59**, 4249 (1999).
- <sup>22</sup> Copley, D. et al. Toward a scalable, silicon-based quantum computing architecture. *IEEE J. Quantum Electron.* **9**, 1552-1569 (2003).
- <sup>23</sup> Braak, D. Integrability of the Rabi Model. *Phys. Rev. Lett.* **107**, 100401 (2011).



- <sup>24</sup> Nataf, P. & Ciuti, C. Protected Quantum Computation with Multiple Resonators in Ultrastrong Coupling Circuit QED. *Phys. Rev. Lett.* **107**, 190402 (2011).
- <sup>25</sup> Romero, G., Ballester, D., Wang, Y. M., Scarani, V., & Solano, E. Ultrafast Quantum Gates in Circuit QED. *Phys. Rev. Lett.* **108**, 120501 (2012).
- <sup>26</sup> Berry, M. V. Quantal Phase Factors Accompanying Adiabatic Changes. *Pros. R. Soc. Lond. A.* **392**, 45-47 (1984).
- <sup>27</sup> Lang, C. et al. Correlations, indistinguishability and entanglement in HongOuMandel experiments at microwave frequencies. *Nature Phys.* **9**, 345348 (2013).
- <sup>28</sup> Helmer, F. et al. Cavity grid for scalable quantum computation with superconducting circuits. *Europhys. Lett.* **85**, 50007 (2009).
- <sup>29</sup> Felicetti, S. et al. Dynamical Casimir effect entangles artificial atoms. Preprint at <http://arxiv.org/abs/abs/arXiv:1402.4451> (2014).

**Acknowledgments** The authors acknowledge support from the National Research Foundation & Ministry of Education, Singapore; Spanish MINECO FIS2012-36673-C03-02; UPV/EHU UFI 11/55; Basque Government IT472-10; and CCQED, PROMISCE, SCALEQIT EU projects.

## SUPPLEMENTARY INFORMATION

### I. THE FLUX QUBIT-CAVITY HAMILTONIAN

The potential energy of a compound flux qubit, shown in Fig. 5, is obtained by combining the corresponding Josephson potentials  $\mathcal{E}(\varphi_\ell) = -E_{J\ell} \cos(\varphi_\ell)$ , where  $E_{J\ell}$  and  $\varphi_\ell$  represent the Josephson energy and the superconducting phase across the  $\ell$ th Josephson junction (JJ). We assume  $E_{J1} = E_{J2} = E_J$ ,  $E_{J3} = \alpha E_J$  and  $E_{J4} = E_{J5} = \beta E_J$ . In addition, the total flux around each closed loop satisfies the flux quantization  $\sum_\ell \varphi_\ell = 2\pi f_\ell + 2\pi n$ , where  $\varphi_\ell$  is gauge-invariant the superconducting phase,  $f_\ell = \phi_\ell/\Phi_0$  is the frustration parameter of the  $\ell$ th JJ, and  $n$  is an integer. The above assumptions lead to the potential energy of both the qubit and the qubit-cavity interaction, that is,

$$\frac{U}{E_J} = - [\cos \varphi_1 + \cos \varphi_2 + \alpha \cos(\varphi_2 - \varphi_1 + 2\pi f_1) + 2\beta(f_3) \cos(\varphi_2 - \varphi_1 + 2\pi \tilde{f} + \Delta\psi)], \quad (5)$$

where  $\beta(f_3) = \beta \cos(\pi f_3)$ ,  $\tilde{f} = f_1 + f_2 + f_3/2$  and  $\Delta\psi$  stands for the phase slip shared by the coplanar waveguide resonator and  $f_2$  loop (see Fig. 5).

We also note that the junction at the central line, JJ6, introduces a boundary condition that modifies the mode structure of the cavity but without modifying the potential equation (5). The latter is provided by the condition that most of the current flows through the cavity<sup>1</sup>. A detailed analysis of an inhomogeneous CWR can be found elsewhere<sup>1,2</sup>. In particular, it has been shown that the phase slip takes the form  $\Delta\psi = \Delta\psi_1(a + a^\dagger)$  where  $\Delta\psi_1 = (\delta_1/\varphi_0)(\hbar/2\omega_r C_r)^{1/2}$ . Here,  $\omega_r$  is the frequency of the first cavity mode,  $C_r$  is the total geometric capacitance of the cavity,  $\varphi_0 = \Phi_0/2\pi$  is the reduced flux quantum, and  $\delta_1 = u_1(x_1) - u(x_2)$  corresponds to the difference between the first-order spatial mode evaluated at points shared by the resonator and the  $f_2$  loop. The potential  $U$  can be further approximated by considering the condition  $\Delta\psi_1 \ll 1$ , which can be satisfied with realistic cavity parameters<sup>1,2</sup>. In this case, we make an expansion of  $\Delta\psi$  term in equation (5) up to second order

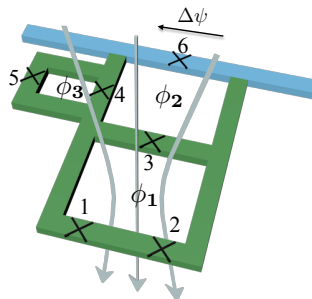


FIG. 5. **Close-up of the flux qubit.** The JJ6 inserted in the central conductor leads to the ultrastrong coupling. The  $f_3$  loop provides switchable qubit-cavity coupling strength.

such that

$$\begin{aligned} \frac{U}{E_J} = & - [\cos \varphi_1 + \cos \varphi_2 + \alpha \cos(\varphi_2 - \varphi_1 + 2\pi f_1) \\ & + 2\beta(f_3) \left[ \cos \tilde{\varphi} \left( 1 - \frac{1}{2!} (\Delta\psi)^2 \right) - \Delta\psi \sin \tilde{\varphi} \right]], \end{aligned} \quad (6)$$

where  $\tilde{\varphi} = \varphi_2 - \varphi_1 + 2\pi f_1$ . From equation (6), we obtain the flux qubit potential  $U_{\text{qubit}} = -E_J(\cos \varphi_1 + \cos \varphi_2 + \alpha \cos(\varphi_2 - \varphi_1 + 2\pi f_1))$  and the tunable qubit-cavity interaction, equation (8). An important feature of the potential, equation (6), is that when  $f_3 = f_1 + f_2 + 0.5$ , the  $\cos(\tilde{\varphi})$  term disappears.

The potential  $U_{\text{qubit}}$  can be diagonalized numerically as a function of the frustration parameter  $f_1$ . In particular, for  $f_1 \sim 0.5$ , the two lowest energy levels are well separated from higher excited energy levels, thus defining a two-level system. After projecting the qubit-cavity interaction into the qubit basis, the system Hamiltonian reads

$$H_{\text{Rabi}} = \frac{\hbar\omega_{eg}}{2}\sigma_z + \hbar\omega_{\text{cav}}a^\dagger a + H_{\text{int}}, \quad (7)$$

with the effective interaction Hamiltonian

$$H_{\text{int}} = -\kappa \sum_{n=1,2} (\Delta\psi)^n \sum_{\mu=x,y,z} c_\mu^n(\alpha, \beta, f_1, f_2, f_3) \sigma_\mu, \quad (8)$$

where  $\kappa = 2E_J\beta(f_3)$  and  $c_\mu^n(\alpha, \beta, f_1, f_2, f_3)$  are the controllable magnitudes of the longitudinal and transversal coupling strengths for  $n$ th order interaction.

When external fluxes satisfy  $f_2 + f_3/2 = 0.5$ , both  $c_y^1$  and the second-order coupling strength are negligible<sup>2</sup>. Thus, the effective interaction Hamiltonian reduces to

$$H_{\text{int}} = \hbar g(a + a^\dagger)(c_z\sigma_z + c_x\sigma_x), \quad (9)$$

where  $c_{z,x} = c_{z,x}^1$  and the switchable qubit-cavity coupling strength  $g = 2E_J\beta(f_3)\Delta\psi^1/\hbar$ .

## II. OPEN SYSTEM ENVIRONMENT

It is unavoidable that any practical and realistic ultrastrong coupling (USC) edges or quantum memory devices (QMDs) operate in noisy environments. Therefore, in this section, we lay down a procedure to treat our system  $H_{\text{Rabi}}$ , equation (7), coupled to a dissipative environment. It is well-known that the standard quantum optics master equation fails in the USC regime<sup>3</sup>. Hence, we follow the perturbative expansion of the system-bath coupling in microscopic derivations and obtain the Redfield quantum master equation<sup>4-6</sup>, that is,

$$\dot{\rho}_{nm}(t) = -i\omega_{nm}\rho_{nm}(t) + \sum_{p,q} \mathcal{R}_{nmpq}\rho_{pq}(t), \quad (10)$$

where

$$\begin{aligned} \mathcal{R}_{nmpq} = & -\frac{1}{2\hbar^2} \sum_{\alpha} \left[ \sum_{v=1}^N (\delta_{mq}\mathcal{B}_{nv}^{\alpha}\mathcal{B}_{vp}^{\alpha}\Gamma_{\alpha}^{pv} + \delta_{np}\mathcal{B}_{qv}^{\alpha}\mathcal{B}_{vm}^{\alpha}\Gamma_{\alpha}^{qv}) \right. \\ & \left. - \mathcal{B}_{np}^{\alpha}\mathcal{B}_{qm}^{\alpha}(\Gamma_{\alpha}^{pn} + \Gamma_{\alpha}^{qm}) \right]. \end{aligned} \quad (11)$$

The tensor  $\mathcal{R}$  depends on the standard damping rate  $\gamma_{\alpha}$  and the transition coefficients  $\mathcal{B}^{\alpha}$  for  $\alpha = r, \sigma_x, \sigma_y, \sigma_z$  with  $r = -i(a - a^\dagger)$ . Here,  $N$  is the dimension of the qubit-cavity system,  $\Gamma_{\alpha}^{ml}|_{m>l} = \gamma_{\alpha}(\omega_m - \omega_l)/\omega_{\text{cav}}$  with  $\omega_{\text{cav}}$  being frequency of the cavity and  $\mathcal{B}_{ml}^{\alpha} = \langle m|\alpha|l\rangle$ . Finally, we define a tensor  $\mathcal{L}$  such that

$$\mathcal{L}_{nmpq} = \delta_{np}\delta_{mq}\omega_{nm} - i\mathcal{R}_{nmpq}, \quad (12)$$

with which we can rewrite our master equation, equation (10), as  $\dot{\rho}(t) = -i\mathcal{L}\rho(t)$ , which has the solution

$$\rho(t) = e^{-i\mathcal{L}t}\rho(0). \quad (13)$$

Therefore, the solution to the open system dynamics of a USC edge can be numerically simulated provided the initial density matrix is known<sup>7</sup>.

### III. CAVITY NETWORK

In order to transfer the state of a qubit along a given path in a cavity network, interactions between neighboring resonators must be selectively turned on and off on demand. This can be done via connecting more resonators to a single circuit node, and then grounding that node through a superconducting quantum interference device (SQUID), as shown in Fig. 6. A SQUID is a superconducting loop interrupted by two Josephson junctions (JJ). When a SQUID is perfectly symmetrical, it behaves as a single JJ, such that its effective Josephson energy can be tuned by threading the loop with an external magnetic flux. Indeed, the SQUID can be seen as a tunable inductance, shunted by a small capacitance. The SQUID inductance can be written as  $L_J = \frac{\varphi_0^2}{E_J(\phi_{\text{ext}})}$ , where  $E_J(\phi_{\text{ext}}) = 2E_J \left| \cos\left(\frac{\phi_{\text{ext}}}{2\varphi_0}\right) \right|$ . Here  $\varphi_0$  is the reduced magnetic flux quantum,  $\phi_{\text{ext}}$  is the external magnetic flux, and  $E_J$  is the Josephson energy.

If the system parameters are chosen in order to make the SQUID impedance way smaller than that of the resonators, the electrical potential at the center of the node can be approximated to zero. Such condition is naturally satisfied in most circuit QED experiments involving SQUIDs in the non-dissipative regime. This enables us to define well separated spatial modes for the electromagnetic field in the different resonators. A direct coupling between resonators is then given by the inductive energy term of the SQUID. The strength of this interaction depends on the SQUID impedance, and so on the external flux threading the device. After quantization, the Hamiltonian describing a single network node can be written as (for details on the derivation see<sup>8</sup>)

$$\mathcal{H} = \hbar \sum_l \omega_l a_l^\dagger a_l - \hbar \sum_{l,r} \alpha_{l,r}(t) (a_l^\dagger + a_l) (a_r^\dagger + a_r), \quad (14)$$

where  $\omega_l$  is the frequency of the  $l$ th resonator and the indexes  $l, r$  run over all resonators pairs. The corresponding coupling parameters are given by

$$\alpha_{l,r}(t) = \frac{\varphi_0^2}{E_J(\phi_{\text{ext}})} \sqrt{\frac{\omega_l \omega_r}{C_l C_r}} \frac{1}{Z_l Z_r}, \quad (15)$$

where  $C_i$  and  $Z_i$  indicate the resonator effective capacitance and impedance, respectively.

When the resonators are off-resonance, i.e. when  $|\omega_l - \omega_r| \gg \alpha_{l,r}$ , their interaction is negligible, as far as the coupling strength is constant. Nevertheless, the SQUID can be driven by an external magnetic flux oscillating at frequencies comparable with that of the resonators<sup>9</sup>. In this way, direct interaction terms between resonator pairs can be tuned on resonance, when the corresponding frequency matching conditions are satisfied. In particular, we can set  $\phi_{\text{ext}}/2\varphi_0 = \bar{\phi} + \Delta \cos(\omega_d t)$ , where  $\bar{\phi}$  is a constant offset and  $\Delta$  is the amplitude of a small oscillation harmonic drive, which frequency is given by  $\omega_d$ . Neglecting terms of the order of  $\Delta^2$  we obtain

$$\frac{1}{E_J(\phi_{\text{ext}})} \approx \frac{1}{\cos \bar{\phi}} + \frac{\sin \bar{\phi}}{\cos^2 \bar{\phi}} \Delta \cos(\omega_d t). \quad (16)$$

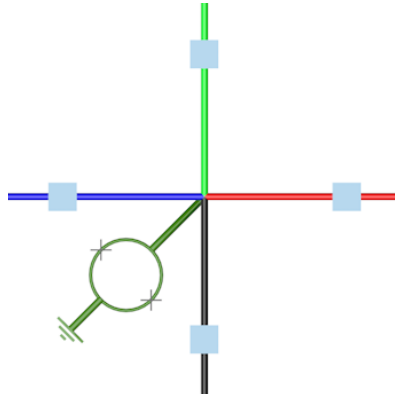


FIG. 6. **A node of the cavity network.** It shows four single-mode resonators grounded through a SQUID device. The colour scheme suggests that the frequencies  $\omega_i$  of the four cavities are different so that direct interactions among them are off-resonance. Hopping interactions between any cavity pair can be activated by driving the SQUID with an external flux, which must be oscillating with the frequency given by the sum of the two cavities bare frequencies.

Hence, to activate hopping interactions ( $a_l^\dagger a_r + a_l a_r^\dagger$ ) between two resonators, the driving frequency must satisfy the condition  $\omega_d = |\omega_l - \omega_r|$ . By controlling the external magnetic flux threading the SQUID device, this scheme allows to selectively turn on an inductive coupling between any two neighboring resonators, which would not interact otherwise.

---

- <sup>1</sup> Bourassa, J. et al. Ultrastrong coupling regime of cavity QED with phase-biased flux qubits. *Phys. Rev. A* **80**, 032109 (2009).
- <sup>2</sup> Romero, G., Ballester, D., Wang, Y. M., Scarani, V. & Solano, E. Ultrafast Quantum Gates in Circuit QED. *Phys. Rev. Lett.* **108**, 120501 (2012).
- <sup>3</sup> Beaudoin, F., Gambetta, J M. & Blais, A. Dissipation and ultrastrong coupling in circuit QED. *Phys. Rev. A* **84**, 043832 (2011).
- <sup>4</sup> Breuer, H.-P. & Petruccione, F. *The Theory of Open Quantum Systems* (Oxford Univ. Press, Clarendon, 2006).
- <sup>5</sup> Ridolfo, A., Leib, M., Savasta, S. & Hartmann, M. J. Photon Blockade in the Ultrastrong Coupling Regime. *Phys. Rev. Lett.* **109**, 193602 (2012).
- <sup>6</sup> Jean, J. M., Friesner, R. A., & Fleming, G. R. Application of a multilevel Redfield theory to electron transfer in condensed phases. *J. Chem. Phys.* **96(8)**, 5827 (1992).
- <sup>7</sup> Nataf, P. & Ciuti, C. Protected Quantum Computation with Multiple Resonators in Ultrastrong Coupling Circuit QED. *Phys. Rev. Lett.* **107**, 190402 (2011).
- <sup>8</sup> Felicetti, S. et al. Dynamical Casimir effect entangles artificial atoms. Preprint at <http://arxiv.org/abs/abs/arXiv:1402.4451> (2014).
- <sup>9</sup> Wilson, C. M. et al. Observation of the dynamical Casimir effect in a superconducting circuit. *Nature* **479**, 376-379 (2011).